An Experimental Study on Shear Behavior of Slurry Infiltrated Mat Concrete Slabs

Liwaa AbdAlhussen [1]*　　　　　　**Layth A. Al-jaberi[2]**

liwaa74.alrbeaa@gmail.com　　　　**dr.laythal-jaberi@uomustansiriyah.edu.iq**

Raid F. Abbas[2]

raid-fadhil-abbas@uomustansiriyah.edu.iq

Abstract: Recently, the Slurry Infiltrated Mat Concrete (SIMCON) has a serious level of attention within civil engineering fields. Within such types of composites, good mechanical properties can be gained if the cement slurry was sprinkled into micro steel fibers matrix. The punching stresses were usually concentrated in a defined parameter as a column reaction against slabs loads and a brittle failure can result. The present study tires investigate the punching shear behavior of SIMCON slabs by conducting an experimental research program. The program included casting and testing of eight SIMCON slabs. The variables of this study focused on, the slab thickness, the volume fraction of micro steel fibers, the propagation nature of micro steel fibers, and the presence/absence of steel reinforcement. The results proved that the punching behavior of SIMCON slabs was more than that of normal concrete slabs. Also, it appears that when the micro steel fibers propagated in all slabs domains, the punching shear behavior was higher than the slabs that micro steel fibers located in in the critical zone of punching only due to the difference in mechanical integrity. In addition, that indicates the first cracking load may reach25.71% in 50mm slabs while it was 10% in 70mm slabs, and the ultimate load increase can reach 49% in 50mm slabs and 26.4% in 70mm slabs.

Keyword: Punching shear; Reinforced concrete slabs; high performance concrete; steel fibers and Brittle failure.

1. Introduction

Reinforced Concrete RC slabs instantly support through columns without the benefit of beams, drop panels, or column capitals. Usually, these slabs were called (flat plates). Such structural elements have various advantages, such as extension spans and a pleasing aesthetic appearance. Flat slab reinforcement is usually simple to install and indicates an acceptable cost option because it minimized the amount of concrete, resulting in fewer dead loads accumulating

---

on foundations. Furthermore, the reduction of stories height, which is a major consequence [1].

In contrast, one of the biggest problems in these types of systems is the punching shear failure (two-way action shear). This failure happens when a portion of concrete (immediately above columns) is pushed out from the slab [2].

Flat slabs may experience punching shear failure, which is brittle and occurs rapidly, potentially resulting in catastrophic failure. As a result, structural designers should consider this issue while designing slabs. However, because the pressures are concentrated, the area directly above the column frequently refer to as the crucial zone. Slurry Infiltrated Mat Concrete (SIMCON) is a new type of concrete that was developed to address the issue of brittleness in some concrete structural elements [4].

The SIMCON usually makes it by organizing enormous amounts of micro steel fibers into a dense network of fibers. After that, a fine particle cement-based slurry or mortar necessities to enter the underground network [5]. SIMCON, on the other hand, can be classified as a distinct type of "Fiber Reinforced Concrete (FRC)." SIMCON differs from FRC in two ways: the volume proportion of steel fibers and the manufacturing process.

In normal FRC, fibers volume fraction is between 1% and 3% by volume according to literature, while in SIMCON, such limit is between 5% and 20% and dependent upon many variables like "diameter", "shape" and "aspect ratio of fibers". SIMCON illustrates "mechanical potential" better than conventional FRC at a moderate steel content [6].

SIMCON's matrix consists of a cement-based fluid with no significant aggregates but a high cement percentage. The fundamental issue is that concrete can contain fine or coarse sand, even if it is made of coarse aggregate. FRC creates by mixing fibers with fresh concrete, whereas SIMCON produces by fully preplacing the fibers within the molds, then the fiber system is infiltrated by cement slurry or flowing mortar. The vibration is applied throughout the running of mortar [7].

The punched shear behavior of typical concrete slabs has been studied extensively in the literature, The essential key components that regulate the punching shear performance of such structural members have been proposed in several recent contributions. Most of these research programs represented their results, interim of empirical equations [8,9,10 and 11]. The influence of moment redistribution has also been explored recently, and it has been demonstrated that

such a limit has a direct impact on the subsequent punching shear behavior [12]. In this field, it was also discovered that the tension reinforcement ratio has a significant impact on the compression reinforcement ratio.[13]. However, some efforts were made to apply numerical modeling using nonlinear finite element analyses, and good agreement with the related experimental data was observed [14].

In addition, several research projects have looked into the punching shear performance of Fibrous Reinforced Concrete (FRC) slabs. Most of these studies focused on the key elements that usually govern the production of FRC like the type / amount of steel fibers and the compressive strength level. It is proved that the presence of 1.5% crimped steel fibers can enhance the relevance punching shear capacity by 30.2%, while the corrugated steel fibers can improve such capacity up to 30% [15,16]. Within the same context, some recent programs proved that if the amount of traditional steel fibers was extended to 60 kg/m3, the consequent improvement in punching shear capacity can reach 39% [17], on the other hand, some researches included numerous attempts to develop credible numerical modeling simulations using a finite element technique, which showed good agreement with current experimental results [18,19].

The main objective of this study is to inspect the punching shear behavior of SIMCON flat slabs and to build a descriptive view about the variation of some important variables that govern the performance of such elements.

Nomenclatures

American Concrete Institute.	ACI
European Federation Dedicated to Specialist Construction Chemicals and Concrete Systems.	EFNARC
European Standard.	EN
High Strength Concrete	HSC
Iraqi Organization Specification.	IOS
Limestone Powder.	L.S.P
Ordinary Portland cement	OPC
Reinforced Concrete.	RC
Slurry Infiltrated Mat Concrete	SIMCON

2. Research Methodology

2.1 Used Materials

2.1.1 Cement

Type I of Ordinary Portland cement (OPC) was used in the present experimental program, the commercial brand of (TASLUJA) was direly stored and tested for physical and chemical properties demonstrated in Tables 1 and Table 2 respectively.

Table 1. Cement physical properties

Property	Results of Testing	Iraqi No.5/1984 specification limits [20]
Blaine fineness (m^2/kg)	405	≥230
"Soundness"	0.35	< 0.8 %
Vicat's Setting Time Initial time (in minutes) Final time (in hours.)	135 3:25	≥45 min ≤ 10 hr
Past Compressive strength 3 days (MPa) 7 days (MPa) 28 days (MPa)	24.4 32.3 47.2	≥15.00 ≥23.00

Table 2. Main compounds / chemical compassion of the used cement

Composition Name	Composition Chemical symbol	Weight %	Iraqi No.5/1984 specification limits [20]
Lime	CaO	61.19	-
Sulfate	SO_3	2.7	<2.80
Silica	SiO_2	21.44	-
Magnesia	MgO	2.31	<5.0
Alumina	Al_2O_3	4.51	-
Insoluble residue	I.R.	0.98	<1.5
Lime saturation factor	L.S.F.	0.84	(0.66-1.02)%
Loss on ignition	L.O.I.	2.39	<4.00
Main compounds (Bogue's equation)			
Dicalcium Silicate	C_2S	29.24	-
Tricalcium Silicate	C_3S	42.83	-
Tetracalcium Aluminoferrite	C_4AF	11.19	-
Tricalcium Aluminate	C_3A	5.73	>5.00

The National Center of Construction Laboratories and Research (NCCLR)

2.1.2 Sand

The sand used throughout the present study is "Al-Ekhaider natural sand" within Karbala governorate is about 2mm maximum size being the fine aggregate within mixes. Table 3 illustrates the grading aggregate used. While Table 4 shows the physical and chemical properties of such sand.

Table 3. Grain size distribution of the used sand

Diameter of Sieve (mm)	Percent of Passing %	Iraqi No.5/1984 specification limits, zone 3 [20]
4.75	97	90-100
2.36	92	85-100
1.18	88	75-100
0.60	71	60-79
0.300	30	12-40
0.150	10	0-10

Table .4 Some fine aggregate chemical characteristics

Properties	Test results	Iraqi No.5/1984 specification limits [20]
Sulfate content	0.09%	≤0.5%
Absolute Specific gravity	2.7	−
Absorption	0.74%	−

2.1.3 Gravel

The crushed gravel in the present experimental program was brought from "AL-Nibaey" within Salah Al-Din Governorate to be used as coarse aggregate within the mix. Such gravel was washed and air dried, then stored in suitable containers until the date of testing. Then, the gravel was saturated "surface dried" before use. Table .5 lists the grain size distribution of that gravel.

Table 5. Grain size distribution of the used gravel

No.	Sieve Size (mm)	Cumulative Passing %	Iraqi No.45/1984 specification limits
1	14	100	100
2	10	100	85-100
3	5.0	18.63	0-30
4	2.36	0.99	0-10

2.1.4 High Range Water Reducing Admixture

This admixture was provided by the Sika Turkish company and is known commercially as "Viscocrete-PC20". Such material is very useful in enhancing the resulted concrete performance and durability and meets the ASTM C494-99 [21] type G and F. Such admixture improves the cement dispersion to a serious concern. Table 6 lists some technical characteristics of such admixture.

Table 6. Some technical characteristics of Viscocrete-PC20

Chemical Base	Modified Polycarboxylate based polymers
Density	Approximately 1.09 -1.13 kg/l at 20°C
Appearance / colors	Light brownish liquid
Viscosity	150MPa
Dosage	1.0-2.0% by weight of cement
Storage Condition	Dry condition at temp. 5°C to 35°C
pH value	3-7

2.1.5 Silica Fume

The grey grade "silica fume" which is a waste material resulted from the fabrication of "silicon" or "ferro-silicon" metal was used throughout the present study. Such materials are also useful material in the reinforced concrete mix if added even in small amounts. The nature of such material is a grey powder that has an appearance like cement of fly ash. The role of silica fume is the "micro filling" process which comprises providing millions of particles that fills the voids within cement paste. In addition to that enhancement role, the resulted calcium hydroxide from the cement hydration can be reacted with silica fume then produced other quantities of "calcium silicate hydrate (C-S-H)". Table .7 lists the physical while Table .8 indicates the "chemical properties" of the used "silica fume", and Table. 9 tabulates the chemical requirements of silica fume according to ASTM C1240-04.

Table 7. Physical properties of the used silica fume*

Physical properties	Analysis	Limit of specification ASTM C1240
Accelerated pozzolanic strength Activity Index with Portland cement at 7days, % of control	128.6	>105
Specific gravity	2.25	--------------------
Percent retained on 45-μm (No.325) sieve	6	<10
Specific surface, m^2	21	>15

*According to the manufacturer.

Table 8. The used silica fume chemical analyses*

Oxide composition	Oxide content %
Al_2O_3	0.01
SiO_2	98.87
CaO	0.23
Fe_2O_3	0.01
Na_2O	0.3
MgO	0.01
K_2O	0.08
Blaine fineness (m^2/kg)	200000

*According to the conformity certificate.

Table 9. Chemical requirements of silica fume ASTM C1240-04

Oxide composition	Analysis %	Limit of ASTM C1240-04
Moisture content	0.68	<3.0
SiO_2	98.87	>85.0
L.O.I	4.02	<6.0

2.1.6 Micro Steel Fibers

The micro steel fibers utilized in the present study are the commercial type that is usually used in domestic cleaning. The diameter of such fibers is 0.5 mm, Figure 1 shows a photograph of the micro-fibers used in the present study.

Figure 1. The micro steel fibers used in the present study

25

2.1.7   Water

All the mixes and the specimen curing were achieved with tap water.

2.1.8   Reinforcing Bars

The deformed bars used throughout the present study are 6mm in diameter. The deformed bars are used for reinforcing the reference slab specimens throughout the present study. The tension test results of such bars are listed in Table 10.

Table 10. Tension tests results for steel bars within this study*

Nominal diameter (mm)	Actual diameter (mm)	Weight (kg/m)	Yield stress (MPa)	Yield strain mm/mm	Ultimate strength (MPa)	Ultimate strain (mm/mm)
6	5.92	0.216	435	0.0023	535	0.165

*Implemented at the College of Engineering, Mustansiriya University

2.2 Mix Proportions

Within this study, the traditional concrete was used to cast the reference beams which are considered as a base for comparison purposes against SIFCON specimens. On the other hand, the other groups were cast with SIFCON. However, both normal and SIFCON mixes were originally selected after many trials mix for ensuring the required properties. Table 11 shows the proposed final mix proportions.

Table 11. The proposed mix proportions

| Mix Type	Mix Proportions					
	Cement kg/m^3	Sand kg/m^3	Gravel kg/m^3	W/C ratio	Silica Fumes	Super Plasticizers l/m^3
"SIFCON"	480	1304	——	230 m^3	144	13
Concrete Strength (30) MPA (N.C)	400	550	1000	0.45	——	——

2.3 Specimens Descriptions

All the specimens are of the total width and length equal to 1000 mm and variable thickness (50mm and 70mm). All the slabs are simply supported at edges at 950mm. The load was applied by a central steel column of 50mm by 50mm cross-section.

In this study, "N" refers to normal concrete in the references that comprise the first group. "S" refers to any SIFCON specimen that contains steel fibers. "F" refers also to a specimen that contains traditional steel fibers while "M" refers to any specimen that had micro steel fibers. Figure (3-4) shows specimens. In addition, "T" referrers to a specimen that contains steel fibers within all the specimen body while "C" refers to a specimen that include steel fibers within the critical zone "a zone that has borders offset of d/2 from column" where d is the "effective depth" of the slab thickness as shown in Figure 2 and Table 12 obtains the specimen details.

Table 12. Designations of Specimens

Group	Slab Designation	Slab Thickness in mm	Traditional Steel Fibers %	Micro Steel Fibers %	Flexural Reinforce.
Group One	N70	70	-	-	Ø6mm at 75mm bottom
	N50	50	-	-	Ø6mm at75mm bottom
Group Two	SF10T70	70	10% T	-	Ø6mm at75mm bottom
	SF10T50	50	10% T	-	Ø6mm at75mm bottom
	SF20T50	50	20% T	-	Ø6mm at75mm bottom
	SF10C50	50	10% C	-	Ø6mm at75mm bottom
	SF10T50*	50	10% T	-	-

Figure 2. Details of slab specimens
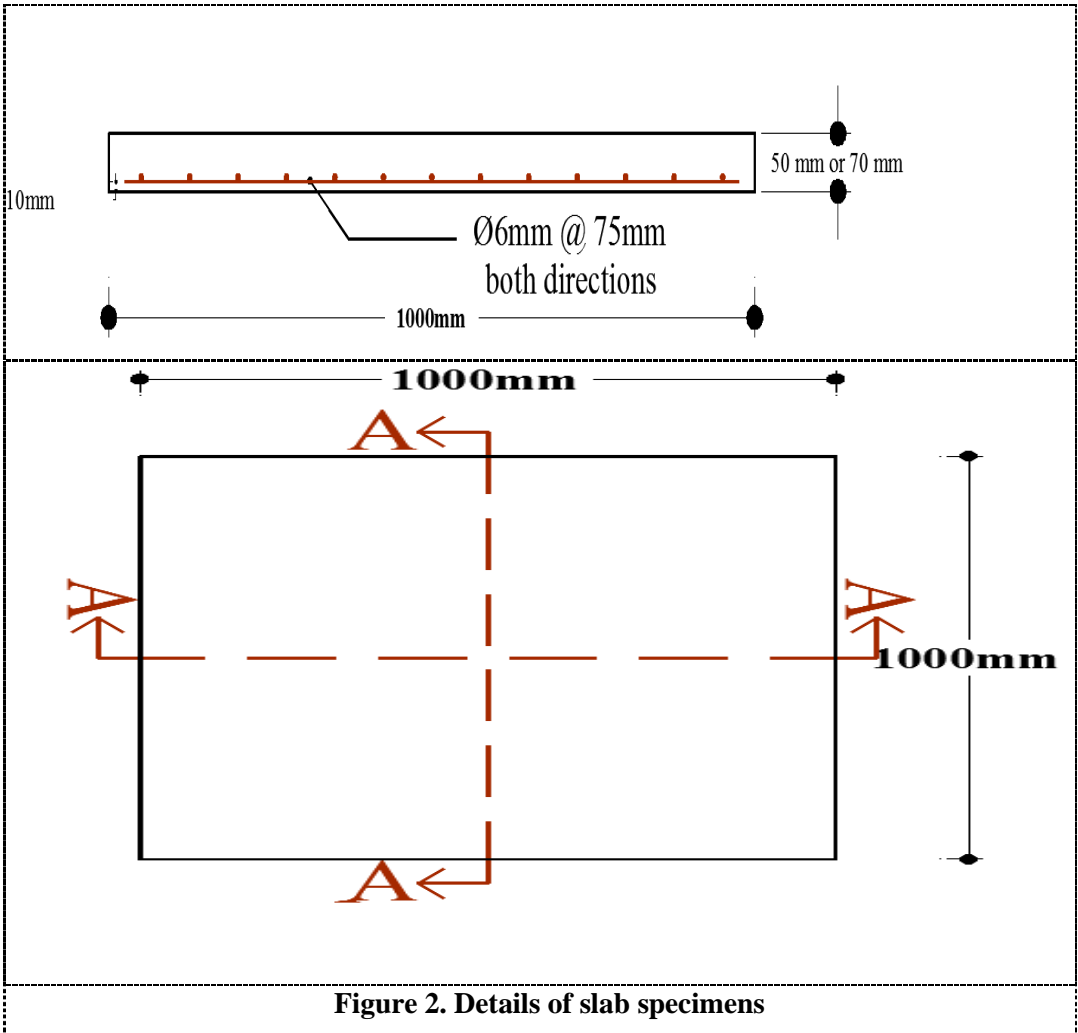
2.4 Mixing Process

In the current study, a rotary laboratory with 0.19 m3 capacity is used for the mixing process. Before starting, a mixer was cleaned suitably to be ready.

The silica fume and the silica sand were mixed in a dry state for 5 minutes. Then, the cement is added to the batch for "5 minutes". Tap water was also added for 2 minutes. Finally, the superplasticizer was added and mixed for an additional 5 minutes.

2.5 Molds of Specimens

The molds used in the casting method with tested specimens of the current study are shown in Figure 4. Such molds consist of a bed and suitable moving sides that can be fastened accurately by appropriate spirals. The "internal edge to edge" dimensions of the molds were (1000 mm x 1000 mm x50 or 70 mm).

2.6 Casting Procedure

Before the casting, the wood forms were ensured to be clean and oiled by (Total Company) car engine oil as shown in Figure 3, then, the selected reinforcement / steel fiber was placed before the concrete/past was added accurately.

After casting, all the specimens were vibrated by electrical tool till the entrapped air was exploded. The "upper surface" was levelled casting surface by using a "steel trowel". To avoid moisture loss, the slab was coated with polyethylene sheets. The specimens were get out of the mold away from molds after 24 hours and stored/cured by tapping after until the testing day.

**Figure 2. Details of slab specimens**
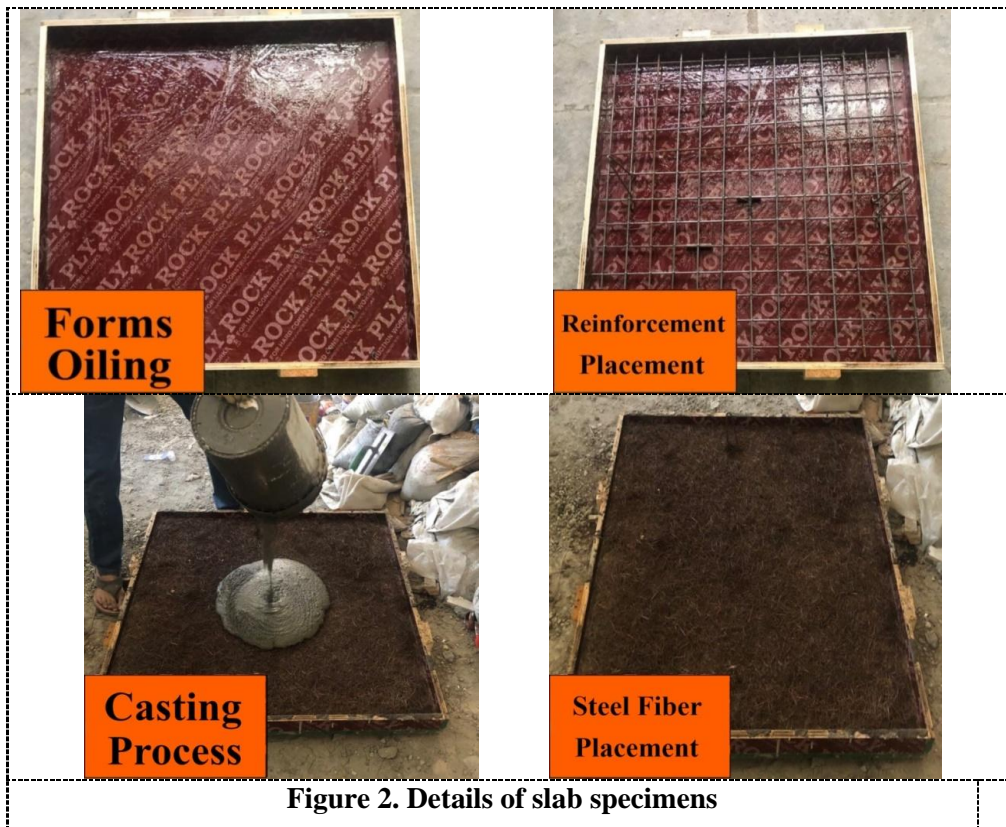
2.7 Punching Test

On the day of testing, the slabs were painted with a (Murgan) white painting to recognize the cracks. Labels containing the slabs designation were also established before the installation of the specimen in the testing machine.

The next step would be the strain gauges and dial gauge linking / establishment and making sure that the testing hydraulic machine is ready for the test. All slabs were tested in the "structural laboratory of the Civil Engineering Department, College of Engineering, Al-Mustansiriya University", using such testing machine of the type (EPP300MFL system) with a capacity of (3000kN) shown in Figure 4. The load incremental order was taken as 5 kN to better recognize the first cracking and the consequent ultimate loading.

Figure 4. The testing of slabs

Figure 5. Testing schematic details
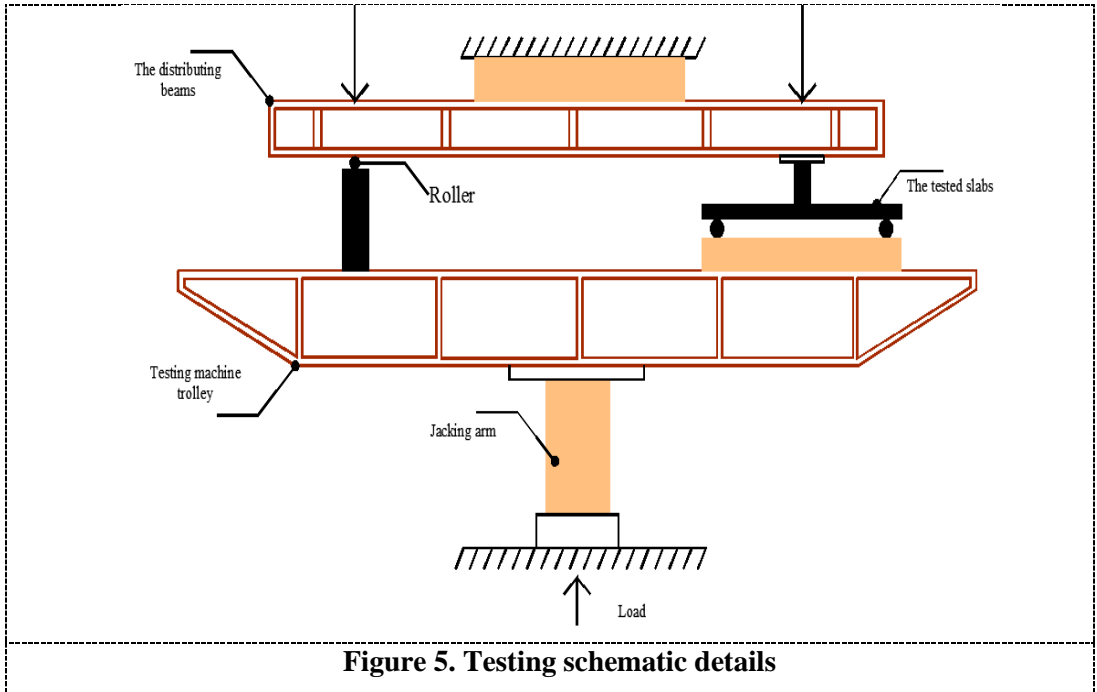
### 2.7.1   Deflection Measurement

The vertical deflection was measured by a dial gauge with an accuracy of 0.01mm that was placed at the "bottom face" of the mid-span of slabs.

2.7.2   Strain Measurements

The 120Ω resistance strain gauge was used to measure at room temperature the strain in the rebar of the specimens. Such strain gauges have the length of 30 mm and width of 10 mm. The steel strain gauges were fixed in the middle top face of the beam specimens. Electrical wires were used to link the strain gauge cells to the digital strain bridge reader, as shown in Figure 7. In addition, Figure 6 shows the strain gauge of concrete while Table 13 shows its properties.

Table 13. Strain gauges properties

Property	Specifications
Width	9 mm
Length	40 mm
Gauge Factor	2.085
Electrical Resistivity	120Ω
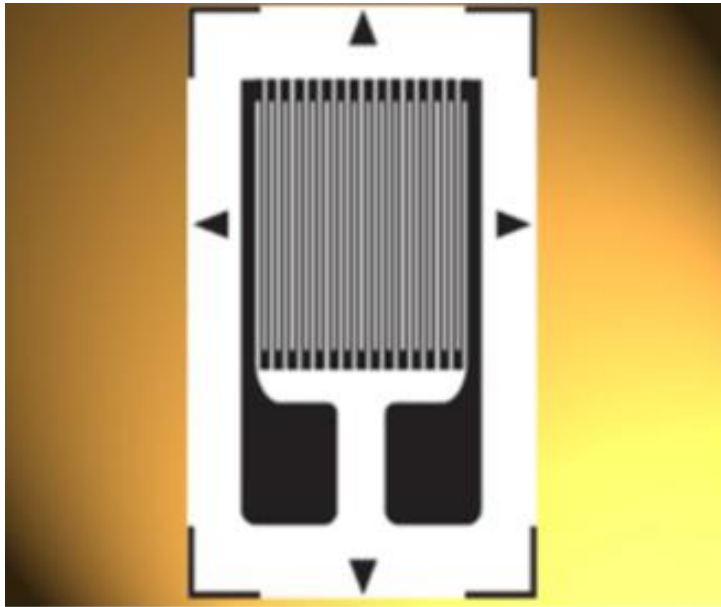
Figure 6. A zoomed view of the strain gauges used in the present study

Figure 7. Data logger device (strain bridges reader)

3. Results and Discussion

Within the current experimental program, fourteen slab specimens were tested. In order to get good understanding under the scope of this work, these specimens were divided into two groups, the first one was devoted to understanding the effect of slab thickness to know how much changing this parameter affects the consequent structural behavior in "normal concrete slabs" and to establish a base point for comparison for the next group. The second group was directed to compare the structural behavior of SIMCON slabs under the proposed conditions of this study.

The structural punching shear behavior within this study is represented in terms of load-deflection relationship, first crack load, yield load, ultimate load, ultimate deflection, steel tensile strain and cracking patterns.

3.1 Structural Punching Shear Behavior of Normal Concrete Slabs: Effect of Slabs Thickness

The structural punching shear behavior of normal concrete slabs is presented in the following sections. The slab specimens that were included in this group are N50 and N70. Such specimens are normal concrete specimens that have 50 mm and 70 mm in thickness respectively.

3.1.1 First Crack Load, Yield Load, and Ultimate Strength

Table 14 shows a comparison between the proposed specimens within this group with respect to "first crack load", "yield load" and "ultimate strength". It can be recognized that the first crack load increased by 14.28% if the slab thickness changed from 50mm to 70mm. Additionally, the relevancy "yield load" increased by 6.39% for the same change as well as an increase in ultimate load strength by10.30 %.

It is obvious that this behavior and difference in first cracking, yielding and ultimate load levels can be ascribed to the excellency of N70 against N50 concerning to the "flexural rigidity".

Table 14. Group one comparison with respect to first crack load, yield load, and ultimate strength

Specimens designation	Cracking load P_{cr} (kN)	Increase in P_{cr} %	Yield load P_y (kN)	Increase in P_y %	Ultimate load P_u (kN)	Increase in P_u %
N50	17.5	/	47	/	82.5	/
N70	20	14.28	50	6.39	91	10.30

3.1.2 Load - Deflection Relationship

Table 15 shows a comparison between the proposed specimens within this group with respect to the yield deflection, ultimate deflection, and ductility ratio for the proposed specimens within this group. It's noticed in Figure (4-6) that the "load – deflection" curves consists of three parts, the first part can be considered as linear elastic as far as "first cracking", the next stage started after the "first cracking" till "yielding of steel reinforcement", while last stage is appeared after such yielding slab "failure" occurs. However, the relevant yield deflection decreased by 28.13% if the slab thickness changed from 50mm to 70mm while the ultimate deflection decreased by 7.18% for the same change.

In addition, Figure 8 shows the load – mid span deflection curves N50 and N70. It can be observed from such figure that N50, illustrated slightly lower stiffness than the N70, while the ductility ratio levels observed 13.63% and 17.18% for N50 and N70 respectively. The high level of ductility ratio for N70 is related to the low level of yielding deflection due to the stiffness supremacy against N50.

Figure 8. Group one load deflection curves
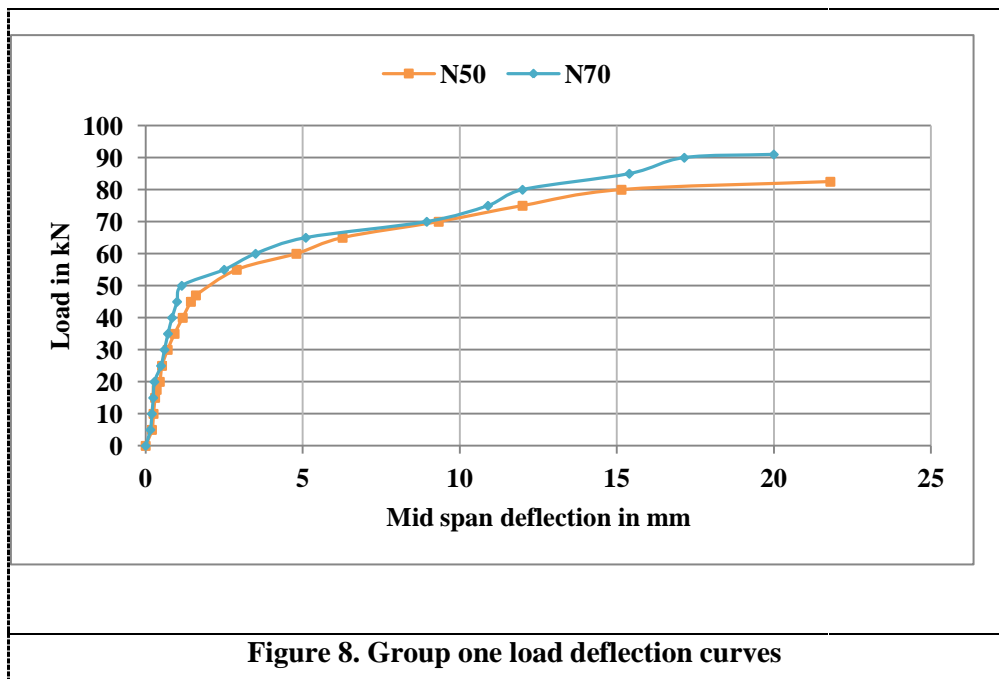
3.1.3 Initial Stiffness

During the present study, the initial stiffness is the slope of the first part of the load-deflection curve. It was calculated by dividing the yield load (Py) to the yield deflection (Δy). The equation used are shown below:

$$Initial\ stiffness = \frac{P_y}{\Delta_y} \tag{1}$$

However, stiffness calculation was carried out according to Sullivan et al., (2004) [22]. The stiffness results for all slab specimens are presented in Table 16. It is observed that the initial stiffness increased 47.99% if the slab thickness changed from 50mm to 70mm. It cleared that this sort was related again to the difference in flexural rigidity between N50 and N70.

Table 16. Initial stiffness for group one

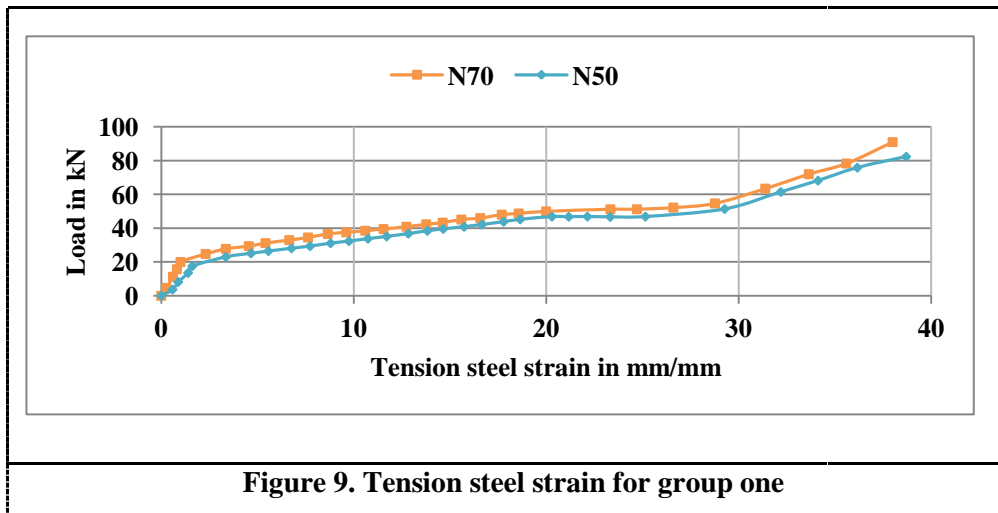| Specimens designation	Yield load P_y (kN)	Yield deflection Δ_y (mm)	Initial Stiffness P_y/ Δ_y (kN/mm)	Increase in Initial Stiffness %
N50	47	1.60	29.38	/
N70	50	1.15	43.48	47.99

3.1.4   Load- Strain Relationship

Table 18 and Figure 10 show a comparison between the proposed specimens within this group with respect to steel tensile strain. It can be distinguished that the "load tension steel - strain diagram" comprises 3 distinct phases; 1st phase is recognized in the region before the first crack limit. The 2nd stage can be registered behind that phase reaching "steel reinforcement yielding" yielding when the effects of slab thickness are visible. The 3rd phase can be seen after that till failure.

The "yielding steel strain" was slightly decreased by 1.43% when thickness of concrete changed from 50mm to 70mm and the ultimate steel strain decreased by 1.84%.

 The reason behind the increase in tensile strain in N50 against can be interpreted again according to the difference in flexural rigidity and the related response in steel reinforcement.

Table 17. Group one comparison with respect to steel tensile strain values

Beam designation	Yield steel strain Ɛy×10000	Decrease in yield steel strain Ɛy %	Ultimate steel strain Ɛu×10000	Decrease in ultimate steel strain Ɛu %
N50	20.30	/	38.70	/
N70	20.01	1.43	37.99	1.84

Figure 9. Tension steel strain for group one

3.1.1   Cracking Pattern

When the test started to N50 and N70, no obvious cracking appeared till the first cracking load listed above. Then after that, the cracks were propagated gradually with increasing the applied load till the sudden failure of punching. The cracks were formed in the middle region and little signs of concrete crushing were also appearing in the middle region of compression face. Figure 10. shows the cracking pattern of the specimens of the current group.

Figure 10. The cracking pattern of group one
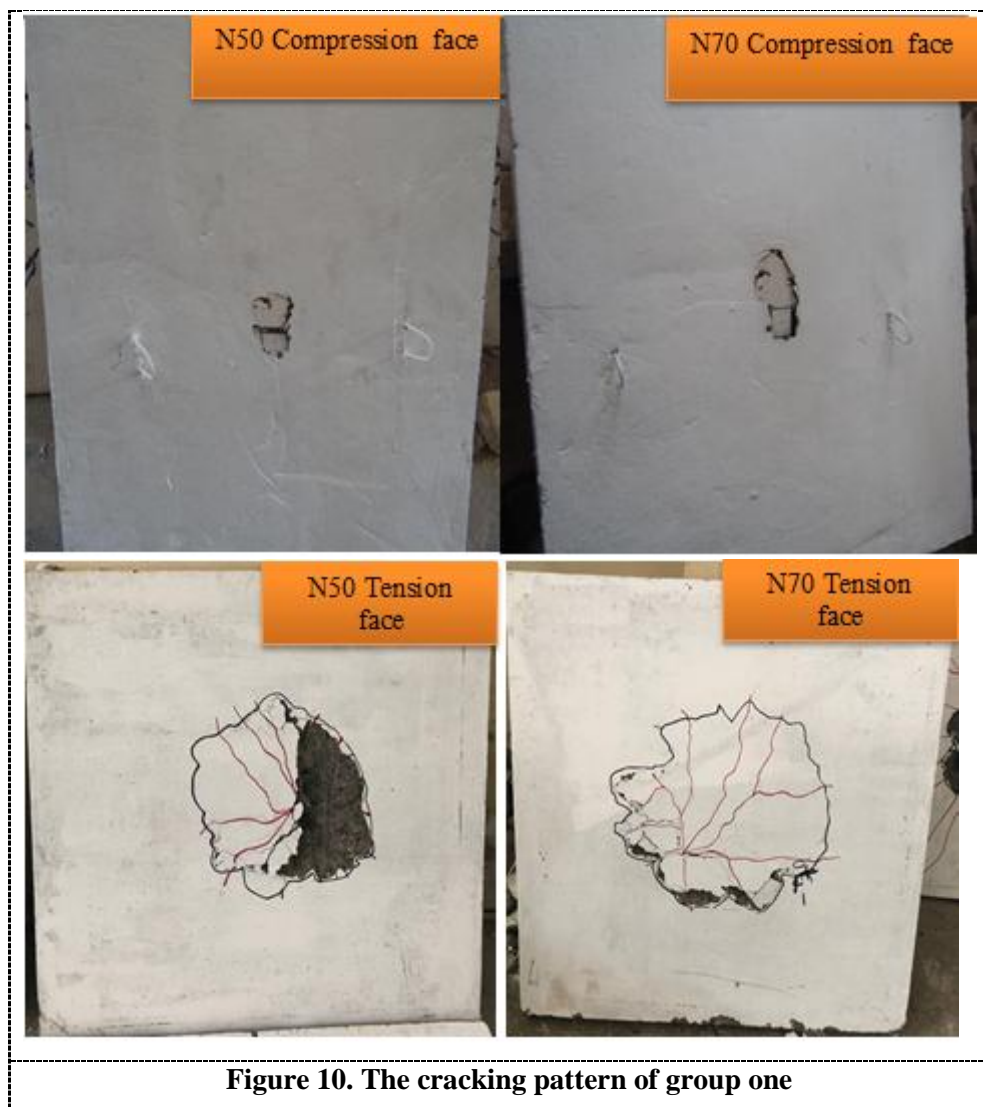
3.2 Structural Punching Shear Behavior of SIMCON Slabs

The structural punching shear behavior of SIMCON slabs is proposed within the next sections. The slab specimens that were included in this group are SM10T50 which is SIMCON slab specimen contained 10% steel fiber spread in total slabs domain and have 50mm thickness. The second specimen is SM20T50 which is SIMCON slab specimen included 20% steel fiber spread in total slabs domain and have 50mm thickness. The third slab is SM10T50* which is SIMCON slab

specimen comprised 10% steel fiber spread in the total slabs domain and have 50mm thickness but have no steel reinforcement. The fourth slab is SM10C50 which is SIMCON slab specimen contain 10% steel fiber spread in the critical punching zone only and have 50mm thickness. The 5th slab is SM10T70, which is SIMCON slab specimen contains 10% steel fiber spread in all slab domain and have 70mm thickness. The 6th slab is SM10C70 which is SIMCON slab specimen consisted of 10% steel fiber spread in a critical punching zone only and have 70mm thickness. As in the previous group, the compression of the above specimens is divided into two categories according to the slab thickness to propose reasonable comparison base points. This compression is made with the specimens of the first group (N50 and N70).

3.2.1   First Crack Load, Yield Load, and Ultimate Strength

Table 18 shows a comparison between the proposed specimens within this group with respect to "first crack load", "yield load" and "ultimate strength". It can be noticed that the first crack load increased by 25.71%, 40, 8.57% and 20% for SM10T50, SM20T50, SM10T50* and SM10C50 respectively. Additionally, the yielding load is also increased by 27.66%, 48.94%, 6.38% and 17.02%, while the ultimate punching shear strength is also changed by +24.24%, +48.48%, -13.93%, and +13.33% for the same set of specimens if compared with the normal concrete (50mm thickness) specimen "N50".

On the other hand, the first crack load increased by 10% and 5% SM10T70 and SM10C70 while the yield load increased by 40% and 20% and the ultimate load increased by 26.37% and 16.49% for the same two specimens if compared with the normal concrete (70mm thickness) specimen "N70". As in the previous group, the micro steel fiber within SIMCON slabs withstand noticeable share of the load in case of full spreading due to the integrity supremacy. In contrast, it is clear that the behavior of SIFCON is better than SIMCON by the general view because the difference in mechanical strength and/or nature of distribution.

The flexural rigidity within this group governs the behavior of steel fiber amounts between SM10T50 and SM20T50 specimen, respectively. The un-reinforced specimen coded as SM10T50 illustrates low behavior after yielding stage if compared with the normal concrete specimen which state that SIMCON does not compensate the main reinforcement as in SIFCON due to its fasciculus nature and the consequent low bridging between concrete fragments after yielding. The priority of flexural rigidity again governs the excellency between SIMCON SPECIMENS regarding crack load, yield load, and ultimate strength for both 50 mm and 70mm comparisons.

Table 18. Group two comparisons with respect to first crack load, yield load, and ultimate strength

Specimens designation	Cracking load P_{cr} (kN)	Increase in P_{cr} %	Yield load P_y (kN)	Increase in P_y %	Ultimate load P_u (kN)	Change in P_u %
50mm slab thickness comparison						
N50	17.5	/	47	/	82.5	/
SM10T50	22	25.71	60	27.66	102.5	+24.24
SM20T50	24.5	40	70	48.94	122.5	+48.48
SM10T50*	19	8.57	50	6.38	71	-13.93
SM10C50	21	20	55	17.02	93.5	+13.33
70mm slab thickness comparison						
N70	20	/	50	/	91	/
SM10T70	22	10	70	40	115	26.37
SM10C70	21	5	60	20	106	16.49

3.2.2   Load - Deflection Relationship

Table 19 shows a comparison between the proposed specimens within this group with respect to the yield deflection, ultimate deflection, and ductility ratio for the proposed specimens within this group.

As in the previous group, it's seen Figure (4-15) that "the load – deflection curves" consists of three stages, the 1st stage is the linear elastic until the first cracking occurrence, the 2nd phase begun beyond elastic part until "yielding of reinforcement", 3rd stage is the stage after yielding of tensile steel reinforcement until the slab punching failure occurs.

However, the relevant yield deflection changed by -14.8%, -3.13%, +25% and -18.13% for SM10T50, SM20T50, SM10T50* and SM10C50 respectively, while ultimate deflection decreased by 9.17%, 35.78%, 4.59% and 6.42 for the same sequence of specimens if compared with the normal concrete (50mm thickness) specimen "N50".

On the other hand, the yield deflection decreased by +73.93%, +66.09%   for SM10T70 and SM10C70 respectively, while the ultimate deflection decreased by 19.55% and 12.15% for the same two specimens above.

In addition, Figure 11 a shows the load – mid span deflection curves for N50, SM10T50, SM20T50, SM10T50* and SF10C50 and the ductility ratio reports 13.63, 6.69, 9.03, 10.40 and 15.57 respectively for that set of specimens within "50 mm thickness comparison" .On the other hand, such ratio observed 17.18, 8.05 and 9.20 for N70, SM10T70 and SM10C70 respectively under "70 mm thickness comparison" as shown in Figure 11 b.
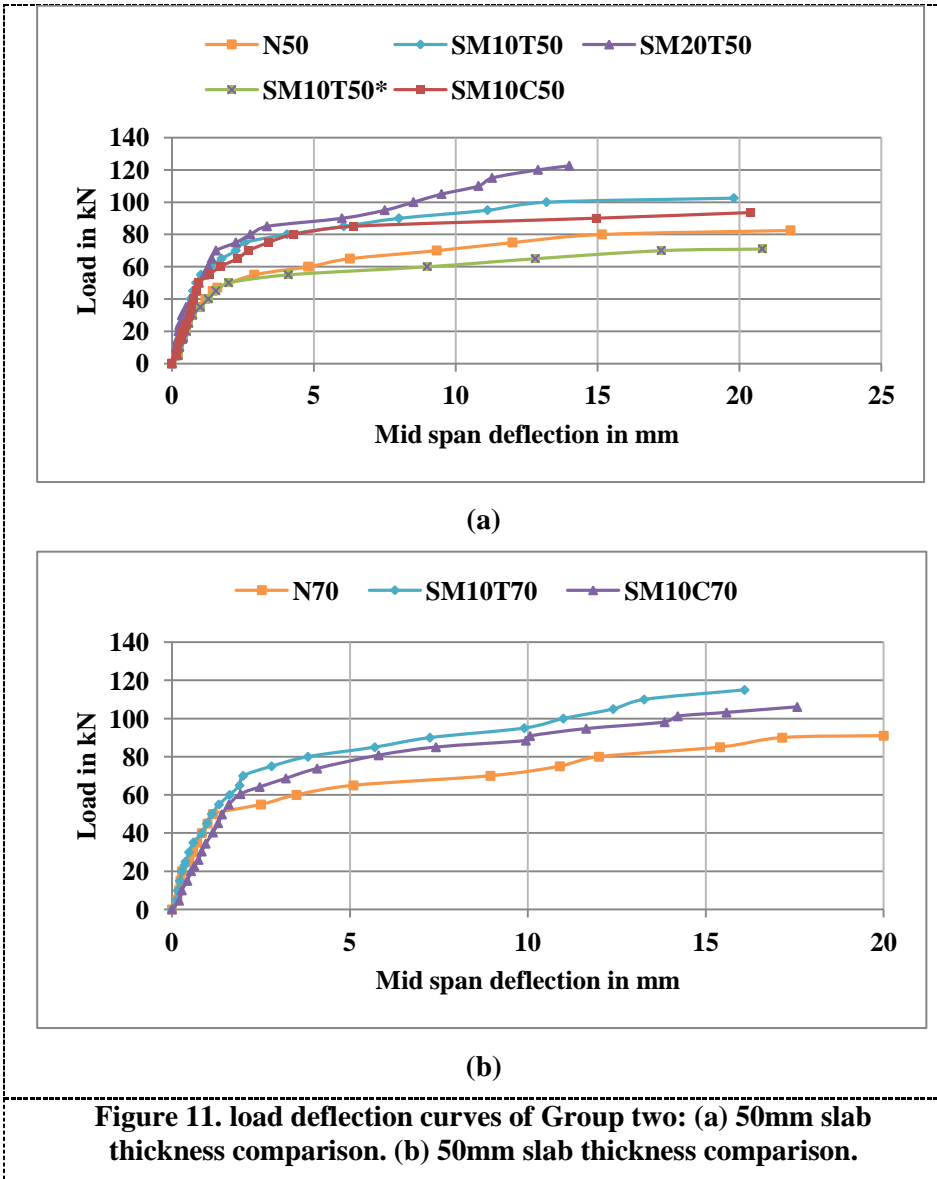
The un-reinforced specimen " SM10T50*" illustrate yielding deflection more than the reference "N50" which confirms the fact that using micro steel fibers for compensating the steel reinforcement is questioned.

Within the 70mm comparisons, the yielding deflection is more than the reference for critical zone and full spreading scenario due to the additional dead load (since the steel reinforcement would not be changed).

However, further research is needed to discover the degree of relation between the (yielding and ultimate) limits of compressive strength stress strain relation and the corresponding limits in mid span curves in SIMCON.

Table 19. Group three comparisons with respect to the yield deflection, ultimate deflection, and ductility ratio

Specimens designation	Yield deflection Δy (mm)	Change in Δy %	Ultimate deflection Δu (mm)	Decrease in Δu %	Ductility ratio $\Delta u/\Delta y$
50mm slab thickness comparison					
N50	1.60	/	21.8	/	13.63
SM10T50	1.37	-14.8	19.8	9.17	6.69
SM20T50	1.55	-3.13	14	35.78	9.03
SM10T50*	2	+25	20.8	4.59	10.40
SM10C50	1.31	-18.13	20.4	6.42	15.57
70mm slab thickness comparison					
N70	1.15	/	20	/	17.18
SM10T70	2	+73.93	16.09	19.55	8.05
SM10C70	1.91	+66.09	17.57	12.15	9.20

(a)

(b)

Figure 11. load deflection curves of Group two: (a) 50mm slab thickness comparison. (b) 50mm slab thickness comparison.

3.2.3   Initial Stiffness

The stiffness results for all slab specimens are presented in Table 20. It is observed that the initial stiffness changed by +49.08%, +53.22%, -14.91% and +42.28% for SF10T50, SF20T50, SF10T50* and SF10C50 respectively if compared with the reference specimen "N50".It is also registered that the initial

stiffness also decreased by -19.50% and -27.76% for SF10T70 and SF10C70 respectively if compared with the reference specimen "N70".

All the initial stiffness of the "un-reinforced specimen SM10T50*" is less than the specimen "N50" which again supports the fact that micro steel fiber was not suitable to compensate the main steel reinforcement.

The initial stiffness increased as the micro steel fiber content. On the other hand, If SM10T50 and SM20T50 specimens were compared with SM10C50, it is noticed again that the "full spread specimen" has an excellency against the "critical punching". The stiffness of SM10T70 and SM10C70 is lower than the reference "N70" due to the high levels of yielding deflection.

Table 20. Initial stiffness for group two

Specimens' designation	Yield load P_y (kN)	Yield deflection Δ_y (mm)	Initial Stiffness P_y/Δ_y (kN/mm)	Change in Initial Stiffness %
50mm slab thickness comparison				
N50	47	1.60	29.38	/
SM10T50	60	1.37	43.80	+49.08
SM20T50	70	1.55	45.16	+53.22
SM10T50*	50	2	25	-14.91
SM10C50	55	1.31	41.98	+42.28
70mm slab thickness comparison				
N70	50	1.15	43.48	/
SM10T70	70	2	35	-19.50
SM10C70	60	1.91	31.41	-27.76

3.2.4   Load- Strain Relationship

Table 21and Figure 12 show a comparison between the proposed specimens within this group with respect to steel tensile strain. As in the previous group, it's seen in Figure 12 that the "load tension steel -strain diagram" comprises three distinct regions; the 1st region was displayed in the area that indicated the

"first crack" limit. The 2nd region is registered after such limit untill the yielding. The 3rd part starts after the previous part when the "diversity" in strain appears more and more to fail after the beginning of "strain hardening".

It is observed that yielding steel strain was also slightly changed by -1.38%, -1.38%, and -1.48% for SM10T50, SM20T50, and SM10C50 respectively, if compared with the reference of 50mm "N50" while the ultimate strain decreased by 13.82%, 9.56% and 7.11% for the same sequence of specimens.

On the other hand, the yielding strain decreased also by 0.95% and 0.70% if compared with the reference specimen "N70" while the ultimate strain decreased also by 13.40% and 9.63% for the same two specimens.
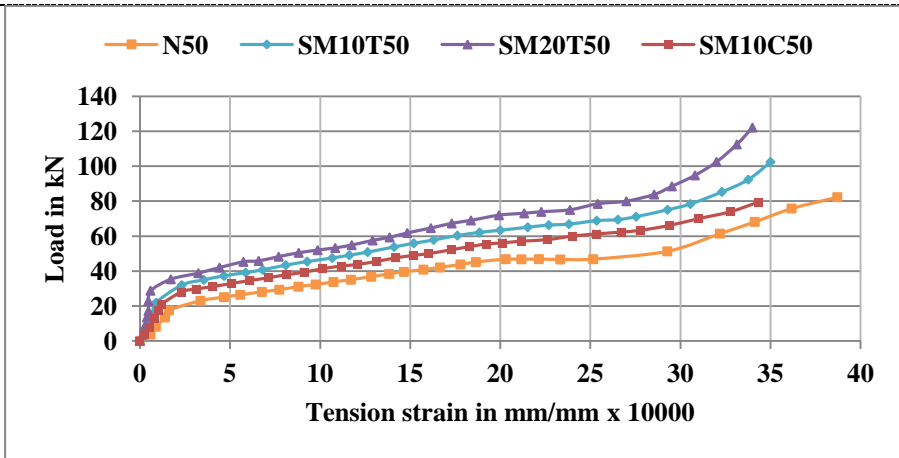
3.2.1   Cracking Pattern

As in the previous group, the cracks began to appear after exceeding the observed cracking load limits and propagated normally to reach "flexural failure".The observed cracks were concentrated in the middle region while the compression face illustrates some additional cracks like the previous group. Figure 13 shows the cracking pattern of the specimens of the current group.
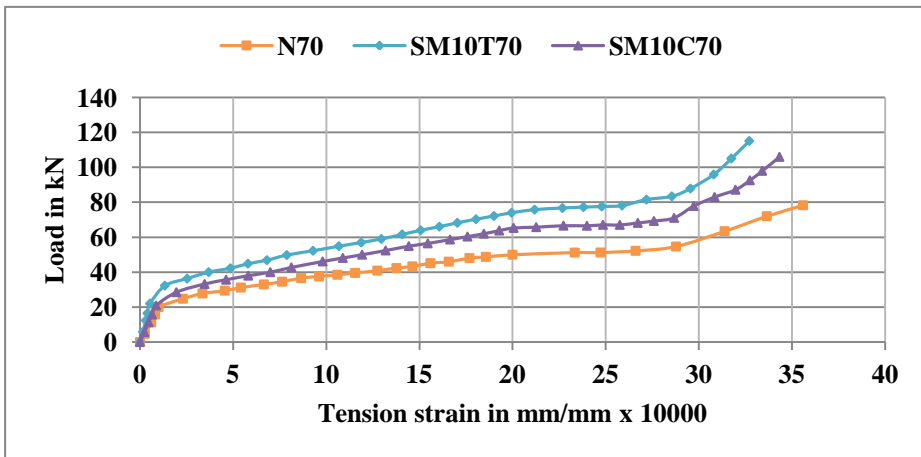
Table 21. Group two comparisons with respect to steel tensile strain values

Beam designation	Yield steel strain $\varepsilon y \times 10000$	Change in yield steel strain εy %	Ultimate steel strain $\varepsilon u \times 10000$	Decrease in ultimate steel strain εu %
50mm slab thickness comparison				
N50	20.30	/	38.70	/
SM10T50	20.02	-1.38	34	13.82
SM20T50	20.02	-1.38	35	9.56
SM10C50	20	-1.48	35.95	7.11
50mm slab thickness comparison				
N70	20.01	/	37.99	/
SM10T70	20.20	0.95	32.71	13.40

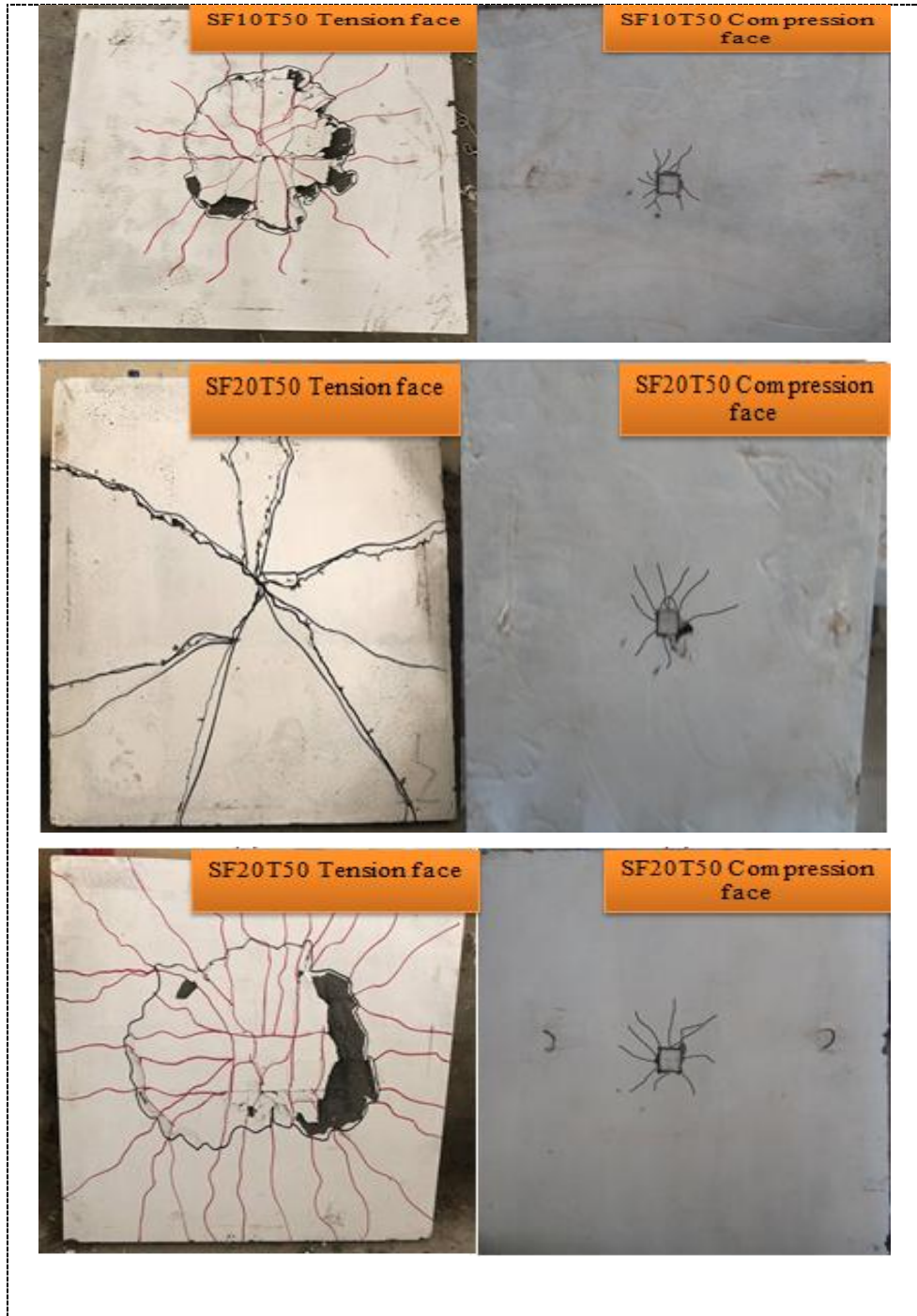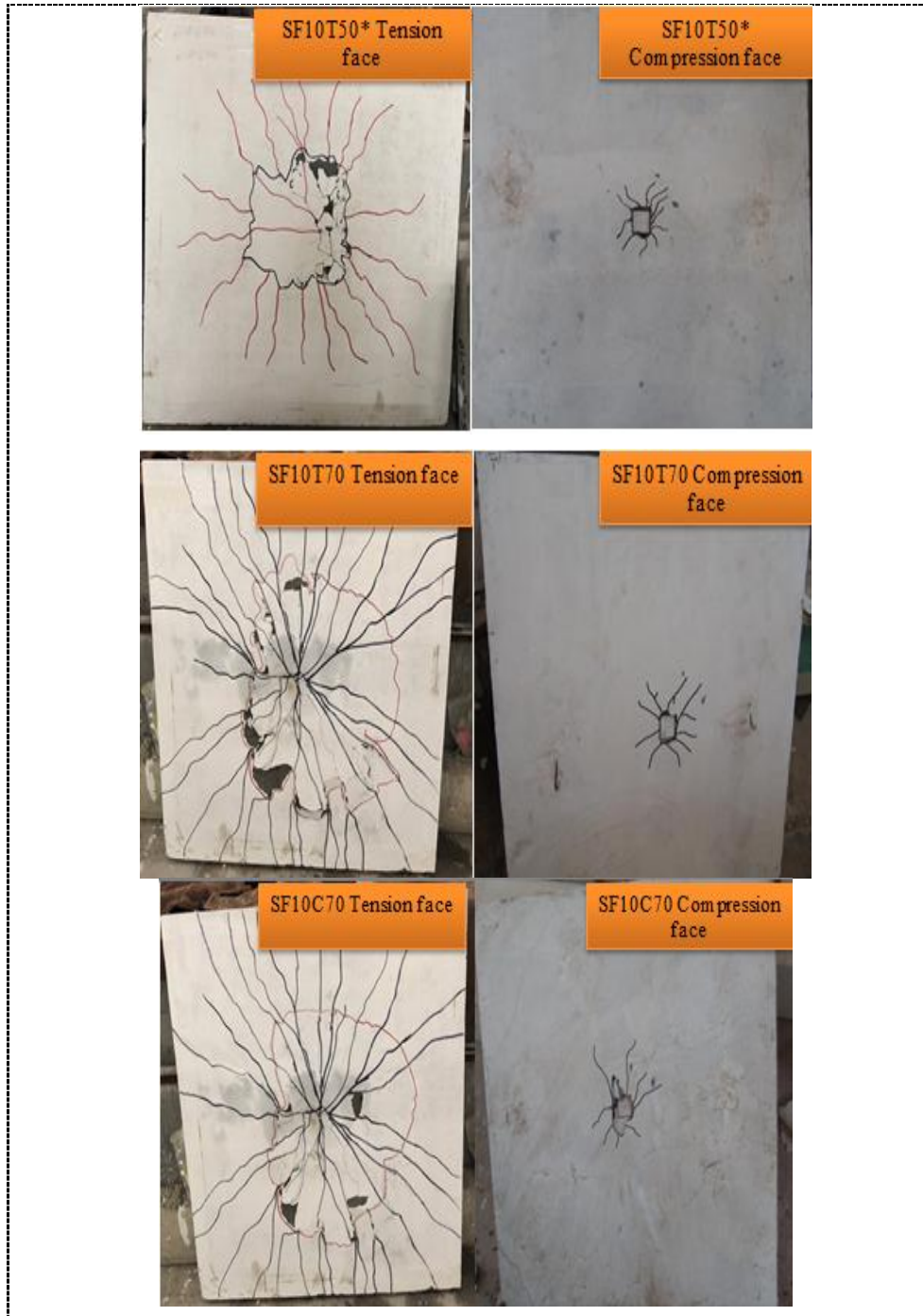| SM10C70	20.15	0.70	34.33	9.63

(a)

(b)

Figure 12. Tension steel strain for group two: (a) 50mm slab thickness comparison. (b) 50mm slab thickness comparison.

Figure 13. Cracking pattern of group two

4. Conclusions

The following were the main conclusions found through the present study

1. The structural behavior of reinforced SIMCON (in general) better than traditional concrete.

2. The use of un-reinforced SIMCON slabs cannot compensate for the traditional reinforced concrete slabs.

3. It was indicated that increasing the steel fiber volume fractions enhanced SIMCON slabs structural behavior.

4. The slabs with steel fibers propagated in all its domain gave better structural behavior, in contrast to an increased propagation with a critical punching zone only due to the difference in integrity.

5. In SIMCON slabs, the first cracking and yielding load are more than traditional concrete slabs.

6. The SIMCON slabs showed a higher first ultimate load than traditional concrete slabs.

7. The first cracking load increase can reach 62.86% in 50mm slabs and 37.5% in 70mm slabs.

8. In SIFCON slabs, obtained an increase in the yielding load up to 29.57% in 50mm slabs and 50% in 70mm slabs.

9. In SIFCON slabs, the ultimate load reached 72.72% in 50mm slabs and 51.10% in 70mm slabs.

5. References

[1] Ying T., (2007) .Behavior and Modeling of Reinforced Concrete Slab-Column Connections , Ph.D. Thesis, The University of Texas at Austin.

[2]   Moe, J. (1961). Shearing Strength of Reinforced Concrete Slabs and Footings Under Concentrated Loads, Portland Cement Association, Research and Development Laboratories, Bulletin D47,April

[3] Yaser, M., Aurelio, M., (2008). Tests on the Post-Punching Behavior of Reinforced Concrete Flat Slabs", Structural concrete laboratory of the Ecole Polytechnique Fédérale de Lausanne (EPFL), Lausanne, Switzerland.1-2.

[4]   Parthiban, K., Saravanara, K., and Kavimukila, G. (2014). Flexural Behaviour of Slurry Infiltrated Fibrous Concrete (SIFCON) Composite Beams. Asian Journal of Applied Sciences, 7 (4), 232–239.

[5] Frazão, C., Barros, J., & Bogas, J. (2019). Durability of Recycled Steel Fiber Reinforced Concrete in Chloride Environment. Fibers, 7 (12).

[6] Naser, F. H., and Abeer, S. Z. (2020). Flexural Behaviour of Modified Weight SIFCON Using Combination of Different Types of Fibers. IOP Conference Series Materials Science and Engineering, 745, 012178.

[7] Ali, A. S., and Zolfikar, R. (2018). Experimental and Numerical Study on the Effects of Size and type of Steel Fibers on the (SIFCON) Concrete Specimens. International Journal of Applied Engineering Research ISSN, 13 (2), 1344-1353.

[8] Yitzaki, D., (1966). Punching Strength of Reinforced Concrete Slabs, ACI Journal, 63 (5), 527-540.

[9] Herzog, M., (1970). A New Evaluation of Earlier Punching Shear Tests. Concrete, London, England, December, 4 (12), 448-450.

[10] Long, A.E., (1975). A Tow-Phase Approach to the Prediction of Punching Strength of Slabs, ACI Journal, 72 (2), 37-45.

[11] Regan, P.E., (1981). Behavior of Reinforced Concrete Flat Slabs, Construction Industry Research and Information Association, CIRIA Report No.89, London.

[12] Choi, J., Kim, J.J., (2012). Experimental Investigations on Moment Redistribution and Punching Shear of Flat Plates, ACI Structural Journal, 109 (3). 329-337.

[13] Said, M., Mahmoud, A. A., and Salah, A. (2020). Performance of reinforced concrete slabs under punching loads. Materials and Structures, 53 (4).

[14] Lewiński, P. M., & Więch, P. P. (2020). Finite element model and test results for punching shear failure of RC slabs. Archives of Civil and Mechanical Engineering, 20 (2).

[15] Ibrahim, J.K., (1984). Punching Shear Strength of Steel Fiber Reinforced Concrete Slabs, M.Sc. Thesis, Baghdad University, 124.

[16] Scott, D.B., Sidney, H.S., (1992). Punching Shear Tests of Concrete Slab-Column Joints Containing Fiber Reinforcement, ACI Structural Journal, 89 (4).425-432.

[17] Minh, L.N., Rovnak, M., Quoc, T.T., Kim, K.N., (2011). Punching Shear Rsistance of Steel Fiber Reinforced Concrete Flat Slabs. The 12th East Asia-Pacific Conference, 14, 1830-1837.

[18] Bastien-Masse, M., & Brühwiler, E. (2015). Experimental investigation on punching resistance of R-UHPFRC–RC composite slabs. Materials and Structures, 49 (5). 1573–1590.

[19] Ju, M., Park, C., Hwang, E. S., & Sim, J. (2015). Predictability evaluation of the existing punching shear formulas using failure test and probability-based approach. KSCE Journal of Civil Engineering, 19 (5). 1420–1430.

[20] Iraqi Specifications No. (5). Portland cement. Baghdad, Iraq. "Iraqi Central Organization for Standardization and Quality Control". Planning Council, Baghdad, Iraq. 1984.

[21]   ASTM C494 / C494M - 99a, "Standard Specification for Chemical Admixtures for Concrete". American Society for Testing and Material. 1999.

[22]   Sullivan, T., Calvi, G., & Priestley, M. (2004). Initial stiffness versus secant stiffness in displacement based design. Paper presented at the 13th World Conference of Earthquake Engineering (WCEE).

دراسة تجريبية لسلوك القص للبلاط الخرساني المصفى المتسلل للطين

ليث الجابري[2]   لواء عبد الحسين[1]
dr.laythal-jaberi@uomustansiriyah.edu.iq   liwaa74.alrbeaa@gmail.com

رائد فاضل عباس[2]
raid-fadhil-abbas@uomustansiriyah.edu.iq

المستخلص: في الآونة الأخيرة ، تتمتع خرسانة السمكون بمستوى جدي من الاهتمام في مجالات الهندسة المدنية. ضمن هذه الأنواع من المركبات ، يمكن اكتساب خواص ميكانيكية جيدة إذا تم رش ملاط الإسمنت في مصفوفة ألياف فولاذية دقيقة. عادة ما تتركز ضغوط قص التثقيب في منطقة محددة وهي رد فعل العمود ضد أحمال البلاطات ويمكن أن ينتج عن ذلك فشل قصيف. تم اجراء الدراسة الحالية للتحقق من سلوك قص التثقيب لبلاطات السمكون من خلال إجراء برنامج بحث تجريبي. تضمن البرنامج صب واختبار ثمانية بلاطات سيمكون. ركزت متغيرات هذه الدراسة على سمك البلاطة، حجم ألياف الصلب الدقيقة ، وطبيعة انتشار ألياف الصلب الدقيقة ، ووجود أو عدم وجود حديد التسليح. أثبتت النتائج أن سلوك التثقيب لبلاطات السمكون كان احسن من سلوك البلاطات الخرسانية العادية. أيضًا ، يبدو أنه عند انتشار ألياف الصلب الدقيقة في جميع مجال البلاطة ، كان سلوك قص التثقيب أعلى من البلاطات التي توجد فيها ألياف الفولاذ الدقيقة في المنطقة الحرجة للتثقيب فقط بسبب الاختلاف في التكامل الميكانيكي. حمل التكسير الأول قد يصل إلى 25.71٪ في بلاطات 50 مم بينما كان 10٪ في بلاط 70 مم ، ويمكن أن تصل زيادة الحمل القصوى إلى 49٪ في بلاطات 50 مم و 26.4٪ في بلاطات 70مم.

الكلمات المفتاحية: قص التثقيب، البلاطات الخرسانية المسلحة، الكونكريت عالي الاداء، الالياف الفولاذية ، الفشل القصيف

---

[1] طالب ماجستير؛ قسم الهندسة المدنية – كلية الهندسة ـ الجامعة المستصرية- بغداد- العراق
[2] استاذ مساعد دكتور؛ قسم الهندسة المدنية – كلية الهندسة ـ الجامعة المستصرية- بغداد- العراق